UNCLASSIFIED

AD 264 544

Reproduced
by the

ARMED SERVICES TECHNICAL INFORMATION AGENCY
ARLINGTON HALL STATION
ARLINGTON 12, VIRGINIA

UNCLASSIFIED

NOTICE: When government or other drawings, specifications or other data are used for any purpose other than in connection with a definitely related government procurement operation, the U. S. Government thereby incurs no responsibility, nor any obligation whatsoever; and the fact that the Government may have formulated, furnished, or in any way supplied the said drawings, specifications, or other data is not to be regarded by implication or otherwise as in any manner licensing the holder or any other person or corporation, or conveying any rights or permission to manufacture, use or sell any patented invention that may in any way be related thereto.

CATALOGED BY ASTIA
AS AD No. 264544

ARPA Order No. 22-59
TASK 5

TG 331-9
Copy No. 22

TASK R

Quarterly Progress Report No. 9
for the period
1 April-30 June 1961

ASTIA
OCT 17 1961
TIPDR

TASK R IS A PROGRAM OF RESEARCH IN BASIC PHENOMENA ASSOCIATED WITH THE BEHAVIOR OF MATERIALS IN HIGH TEMPERATURE GAS ENVIRONMENTS. IT IS SUPPORTED BY THE ADVANCED RESEARCH PROJECTS AGENCY THROUGH CONTRACT NORD 7386 WITH THE BUREAU OF NAVAL WEAPONS, DEPARTMENT OF THE NAVY.

Released to ASTIA by the
Bureau of NAVAL WEAPONS
without restriction.

XEROX

THE JOHNS HOPKINS UNIVERSITY
APPLIED PHYSICS LABORATORY
8621 GEORGIA AVENUE SILVER SPRING, MARYLAND

ARPA Order No. 22-59
TASK 5

TG 331-9

TASK R

Quarterly Progress Report No. 9
for the period
1 April-30 June 1961

THE JOHNS HOPKINS UNIVERSITY
APPLIED PHYSICS LABORATORY
8621 GEORGIA AVENUE SILVER SPRING, MARYLAND

GENERAL OBJECTIVES OF TASK R

Many of the wide variety of problems associated with the use of materials at high temperatures occur in connection with advanced propulsion systems, and of these, some of the most critical and complex are encountered in high performance rocket motors. Present trends in rocket design and propellant formulation resulting in gas flows of increased temperature, pressure, and corrosiveness may be expected to aggravate the materials situation. It seems self-evident that future, long-range solutions to these problems must relay on more sophisticated approaches and broader knowledge of the behavior of materials in high temperature gas environments than is characteristic of the usual "quick-fix", or expensive cut-and-try test procedures. It also seems likely that improvement in structural materials themselves (i.e., higher strength at high temperature, higher melting point, etc.) has reached the point of diminishing returns, so that various other subterfuges must be tried.

Research performed under Task R at the Applied Physics Laboratory or its subcontracting agencies is intended to provide some of the fundamental knowledge necessary for a rational understanding of the behavior of materials at high temperatures. This is a very broad and very complex field involving many different scientific disciplines. While no attempt is made to rigidly limit the scope of Task R, the general emphasis is on appropriate research in the flow and physical chemistry of high temperature gases such as are characteristic of advanced solid propellant rocket motors, and the phenomena basic to heat transfer and cooling techniques in such environments, rather than in the properties of materials themselves.

A. A. Westenberg
Program Coordinator

SUMMARY

I. THERMAL CONDUCTIVITY OF GASES

(N. deHaas and A. A. Westenberg)

Objective

The analysis of the problem of convective heat transfer both in the laminar and turbulent flow regimes requires that the properties of the gases involved be quantitatively understood. The coefficient of thermal conductivity is one such property. Measurement of thermal conductivity of gases has not been a forsaken field of research, and several common gases have been investigated up to temperatures approaching reaction motor temperatures. The primary shortcomings of past and present research in the study of thermal conductivity of gases for application to such heat transfer problems are: a) Inability to apply present experimental methods to temperatures above about 1000°K (most measurements are made at substantially lower temperatures than this), b) the complexity and difficulty in using the usual apparatus for this measurement (thermal-conductivity cells), and 3) the lack of measurements of species (and mixtures) prevalent in reaction motors. Other shortcomings could be listed.

Recent measurements of molecular diffusion coefficients - a closely related transport property - of common flame gases at temperatures in excess of 1000°K applied a simple concept (Ref. 1) that could, in principle, be used for measuring other gas transport properties (conductivity and viscosity). In this method, a point source of a trace gas is located in the center of a uniform, heated laminar jet of a second gas. A series of gas samples removed immediately downstream of the source and quantitatively analyzed is used to determine the molecular diffusion coefficient. The technique has good precision (+1-2%) and is quite adaptable to high temperatures and various gas types.

Adaptation of this method to the measurement of thermal conductivity of gases is an obvious extension. The source of trace gas is replaced with a line source of heat and the temperature rise downstream of the heat source is measured with an appropriate technique. The method is simple, should have good precision, and can be used with a variety of gases at high ambient temperature (approaching flame temperatures). Thus, the objective of this research is to develop the line-source technique for the measurement of gas thermal conductivity, and to use the method of obtaining data over a wide range of temperature on pure gases and mixtures of propulsive interest.

Apparatus

Previous reports (Refs. 2,3) in this series have mentioned the use of an absolute low-speed anemometer to measure the velocity of the gas stream in the region of the thermal wake measurements. For simplicity, it was desirable to use the same wire as the A.C. heat source required in the velocity measurement (Ref. 4) as well as the D.C. line source for the thermal wake width measurement. For various reasons, an A.C. frequency of 100 cps was the most convenient and satisfactory for pulsing the wire during the anemometer measurement. This meant that the wire had to be less than 1 mil diameter in order to follow the 100 cps signal adequately. A common source (Pt or Pt-10% Rh) of 0.5 mil diameter was used satisfactorily for a number of runs in the temperature range 294°K to 1050°K. There was a difficulty however. Although provision was made for tightening the wire, a sufficient amount of tension could not be placed

on the 1.5 in. long source to prevent it from oscillating at the higher temperatures. Attempts to place sufficient tension on the source usually broke the wire, and considerable time was lost in replacement.

Consequently, it was decided to use a stronger 1-mil wire for the line source, and a separate 0.5 mil source for the velocity determination, since the latter would not have to be more than a few millimeters long and therefore would have much less tendency to oscillate. The velocity source was made from Wollaston wire mounted on a set of wire prongs which may be located at various points along a diameter across the jet. This source has provided good temperature signals to the hot-wire pickup at jet temperatures as high as 1064°K in N_2. The pickup is a 2mm dissolved portion of 0.0001 in. Pt Wollaston wire which is also mounted on a set of wire prongs. These prongs are attached to the three-dimensional movement on which the thermocouple is mounted.

One of the following sections gives some results on the measurement of the thermal conductivity of mixtures of N_2 and CO_2. The mixtures were prepared by passing the separate gases through calibrated critical orifices and then into a common chamber before entering the furnace. The mixture proportions were continuously monitored with a thermistor thermal-conductivity cell which was calibrated to give the mole fractions of the component gases.

The temperature of the jet gases is measured with a 0.001 in. Pt, Pt-10% Rh thermocouple. With regulated gas flow through the furnace and regulated current through the two furnace coils, the jet temperature will remain constant to ± 1°K for a period of several hours. This degree of stability is more than adequate for the measurements that are required.

Theory of the Thermal Conductivity of Binary Polyatomic Gas Mixtures

This section presents a summary of the theory of the thermal conductivity of a mixture of two polyatomic gases and specifies certain quantities used in the next section.

The thermal conductivity of a mixture of two polyatomic gases as derived by Hirschfelder (Ref. 5) is given by

$$\lambda_m = \lambda_m^o + \frac{\lambda_1 - \lambda_1^o}{1 + \frac{x_2}{x_1}\frac{D_{11}}{D_{12}}} + \frac{\lambda_2 - \lambda_2^o}{1 + \frac{x_1}{x_2}\frac{D_{22}}{D_{12}}} \tag{1}$$

In this equation λ_m and λ_m^o are the thermal conductivity and the translational (i.e., with internal degrees of freedom frozen) thermal conductivity of the mixture, respectively, λ_i and λ_i^o are similarly defined for the pure components i (i = 1,2), x_i are the mole fractions, D_{12} is the binary diffusion coefficient, and D_{ii} are the self-diffusion coefficients of the pure components.

The translational thermal conductivity of a mixture has been given by Muckenfuss and Curtiss (Ref. 6; see also Ref. 7) and is as follows for two components:

$$\lambda_m^o = 4\,\frac{x_1\,x_2\,(L_{12} + L_{21}) - x_1^2\,L_{22} - x_2^2\,L_{11}}{L_{11}\,L_{22} - L_{12}\,L_{21}} \tag{2}$$

where

$$L_{11} = -\frac{4x_1^2}{\lambda_1} - \frac{16T}{25P}\,x_1\,x_2\,\frac{\frac{15}{2}M_1^2 + \frac{25}{4}M_2^2 - 3M_2^2 B_{12}^* + 4M_1M_2A_{12}^*}{(M_1 + M_2)^2\,D_{12}}$$

$$L_{22} = -\frac{4x_2^2}{\lambda_2} - \frac{16T}{25P}\,x_1\,x_2\,\frac{\frac{15}{2}M_2^2 + \frac{25}{4}M_1^2 - 3M_1^2 B_{12}^* + 4M_1M_2A_{12}^*}{(M_1 + M_2)^2\,D_{12}}$$

and

$$L_{12} = L_{21} = \frac{16T}{25P} x_1 x_2 M_1 M_2 \frac{\frac{55}{4} - 3B^*_{12} - 4A^*_{12}}{(M_1 + M_2)^2 D_{12}} .$$

In these equations M_i are the molecular weights, T is the temperature, P is the pressure, and A^*_{12} and B^*_{12} are the usual dimensionless ratios of collision integrals (Ref. 8) for the particular intermolecular potential function being used. The Lennard-Jones (6-12) potential was assumed here.

In the calculation of λ_m for mixtures of N_2 and CO_2, λ^o_i and D_{ii} were computed from viscosity data on the pure components (Ref. 9) using

$$\lambda^o_i = (15/4)(R/M_i) \eta_i \qquad (3)$$

$$D_{ii} = (6A^*_{ii}/5\rho_i) \eta_i \qquad (4)$$

where η_i are the viscosities, ρ_i the densities, and A^*_{ii} the usual collision integral ratios for the pure components. The pure component thermal conductivities λ_i were the experimental values obtained in this work, while the binary diffusion coefficients D_{12} had been measured earlier in this Laboratory (Ref. 10). The ratios of the collision integrals were obtained for the Lennard-Jones (6-12) model using $(\epsilon/k)_{12}$ = 154°K (Ref. 10), $(\epsilon/k)_{CO_2}$ = 213°K, and $(\epsilon/k)_{N_2}$ = 79.8°K (Ref. 8).

Results

Measurements of the thermal conductivity of nitrogen and carbon dioxide by the line source technique in the temperature range from 300° to about 1000°K are given in Figs. I-1 and I-2. Results by other investigators are also given. It will be seen that the agreement is generally good,

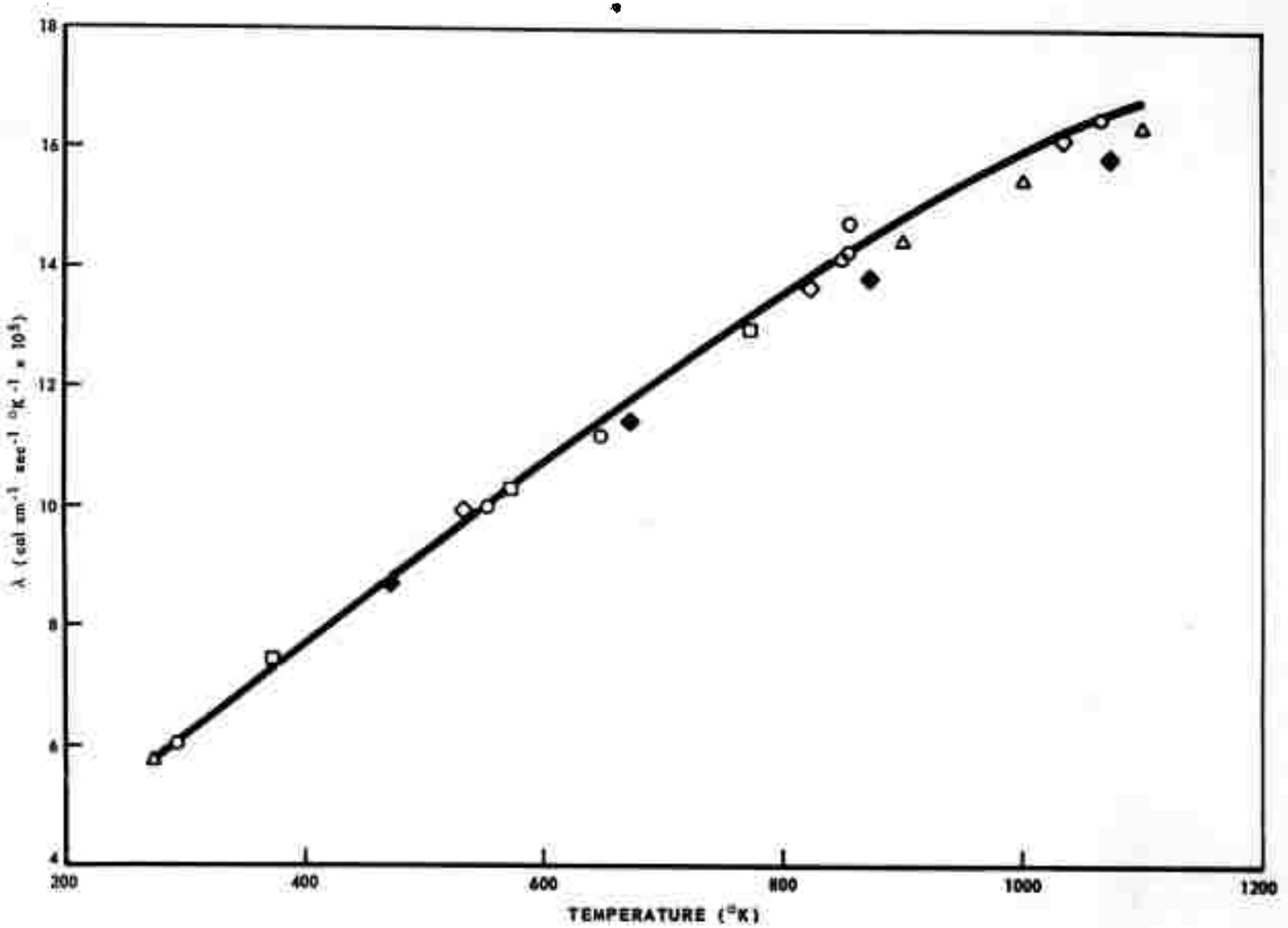

Fig. I-1 COMPARISON OF MEASUREMENTS OF THERMAL CONDUCTIVITY OF NITROGEN WITH VALUES REPORTED IN THE LITERATURE

○ - this work; □ - Nuttall and Ginnings (11);
△ - Stopa (12); ◇ - Vines (13);
◆ - Rothman and Bromley (14).

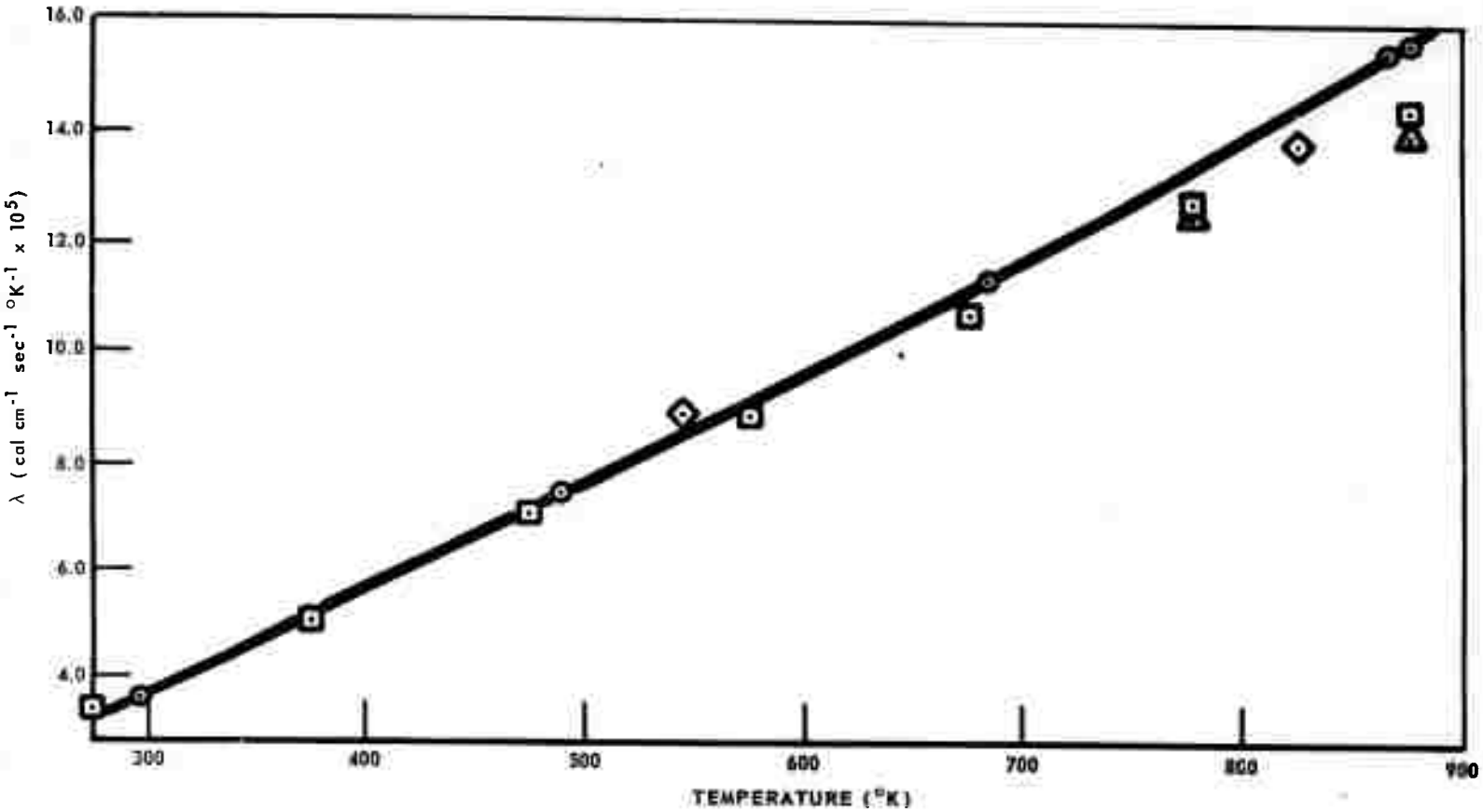

Fig. I-2 COMPARISON OF MEASUREMENTS OF THERMAL CONDUCTIVITY OF CARBON DIOXIDE WITH VALUES REPORTED IN THE LITERATURE

⊙ = this work; ◇ = Vines (13); ⊡ = Vargaftic and Oleschuk (15); △ = Rothman and Bromley (14).

although at the higher temperatures there appears to be an appreciable discrepancy for CO_2. Whether this is real or not remains to be seen - the data are being checked.

Fig. I-3 shows similar data for a 50-50 mixture of N_2 and CO_2. Mixtures containing 25% and 75% N_2 are also being measured and the data are nearing completion. Fig. I-4 gives a comparison of measured and theoretical values for the binary mixtures over the range of composition at two different temperatures. The theoretical curves were obtained as outlined in the previous section, while the experimental values were taken from the λ_m vs. T curves of the appropriate mixtures. It is apparent that theory and experiment are in good agreement at 550°K but not at room temperature. The significance of this, if any, awaits further checking and study before any interpretation will be attempted.

References

1. R. E. Walker and A. A. Westenberg, J. Chem. Phys. 29, 1139 (1958).

2. Task R Quarterly Progress Report No. 7, 1 October - 31 December 1960, The Johns Hopkins University, Applied Physics Laboratory Report No. TG-331-7.

3. Task R Quarterly Progress Report No. 8, 1 January - 31 March 1961, The Johns Hopkins University, Applied Physics Laboratory Report No. TG-331-8.

4. R. E. Walker and A. A. Westenberg, Rev. Sci. Inst. 27, 844 (1956).

5. J. O. Hirschfelder, Sixth International Combustion Symposium, Reinhold Publishing Corporation, New York, 1957, p. 351.

6. C. Muckenfuss and C. F. Curtiss, J. Chem. Phys. 29, 1273 (1958).

7. E. A. Mason and S. C. Saxena, Phys. of Fluids 1, 361 (1958); J. Chem. Phys. 31, 511 (1959).

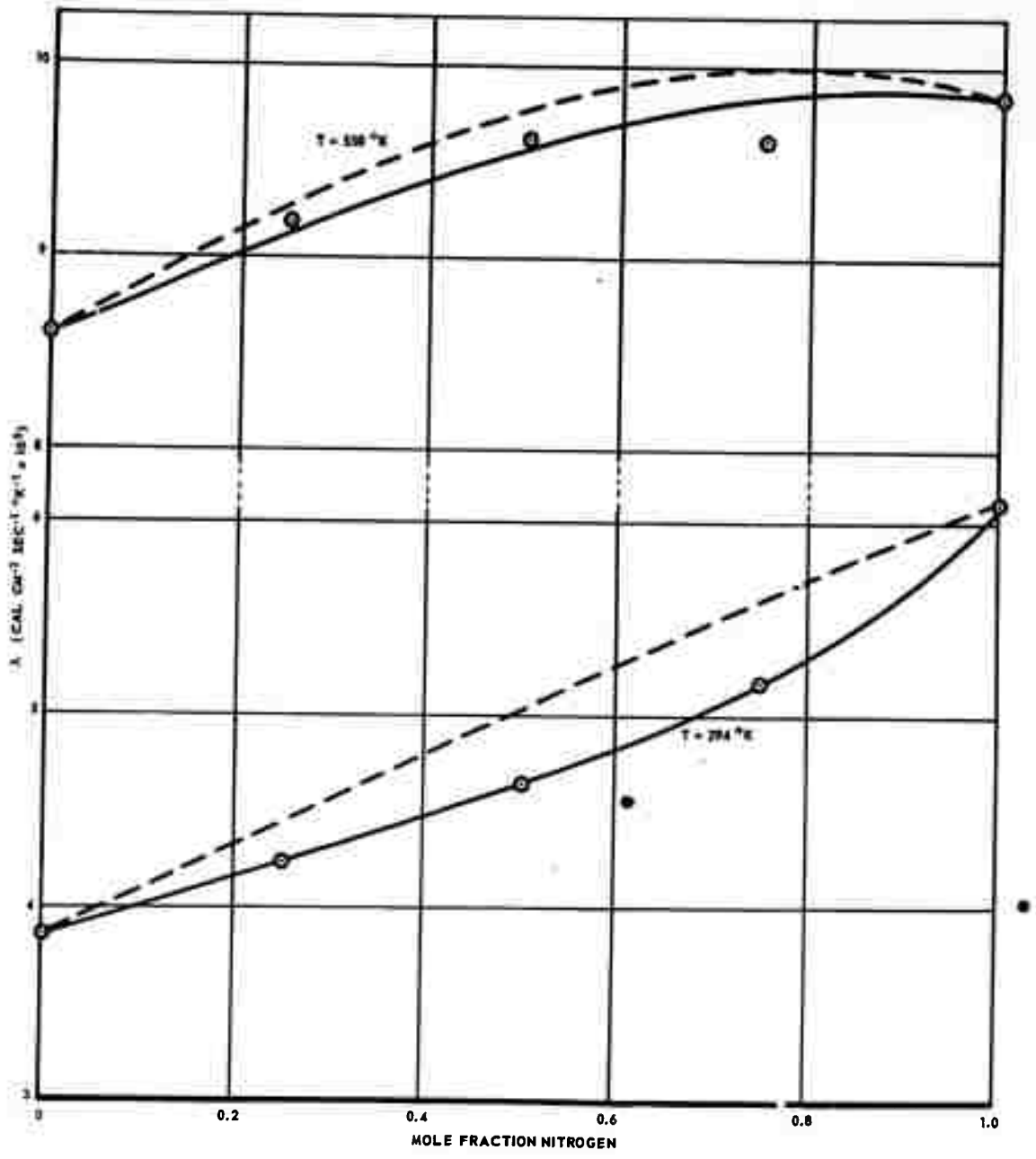

Fig. I-3 MEASUREMENTS OF THERMAL CONDUCTIVITY OF MIXTURE OF 50 MOLE PER CENT NITROGEN -- 50 MOLE PER CENT CARBON DIOXIDE

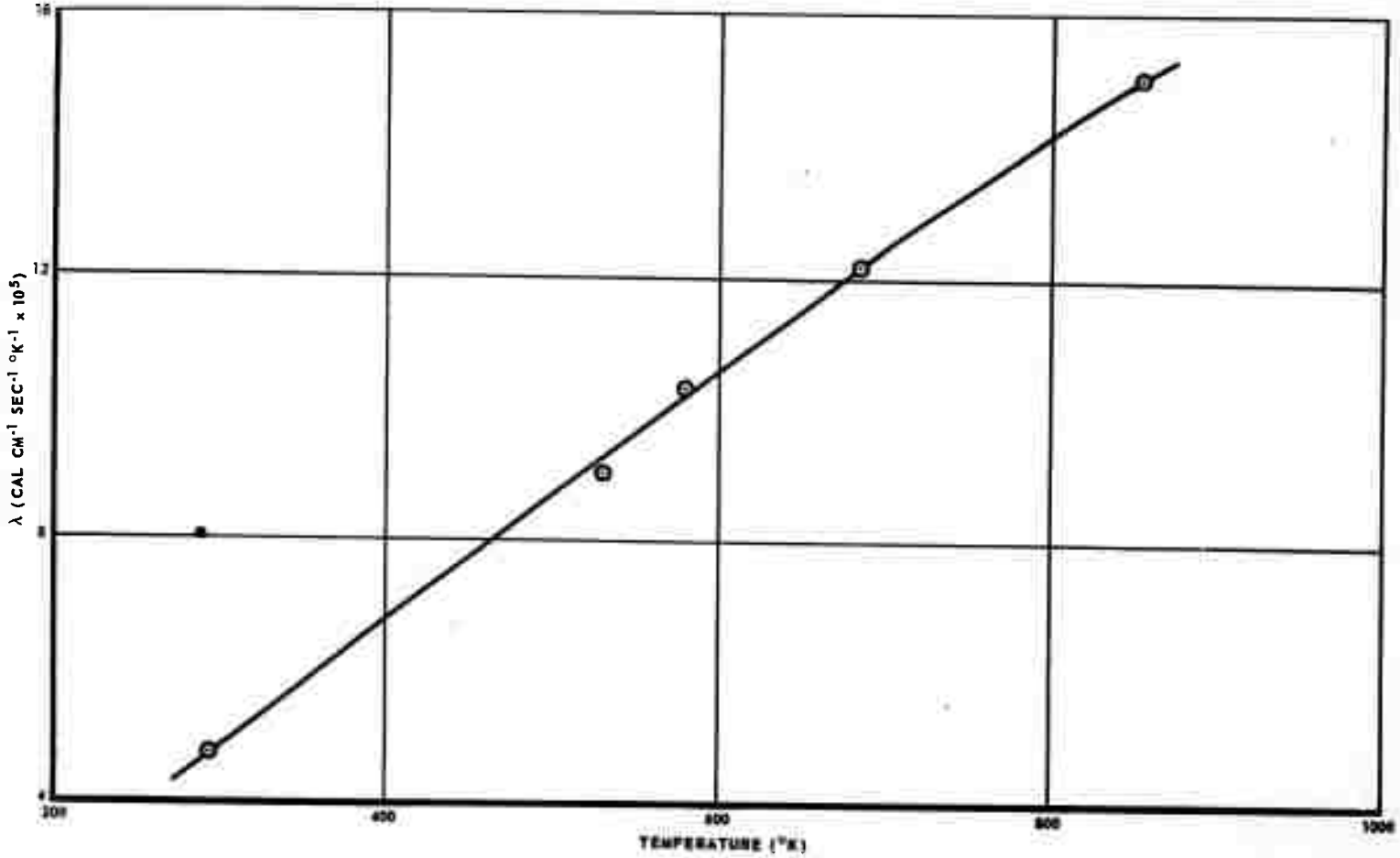

Fig. I-4 COMPARISON OF THEORETICAL THERMAL CONDUCTIVITY OF MIXTURES OF NITROGEN AND CARBON DIOXIDE WITH EXPERIMENTAL MEASUREMENTS

Indicated points have been taken from a smoothed plot of measured λ versus T.

8. J. O. Hirschfelder, C. F. Curtiss, and R. B. Bird, Molecular Theory of Gases and Liquids, John Wiley & Sons, Inc., New York, 1954.

9. J. Hilsenrath, et al, Tables of Thermodynamic and Transport Properties, Pergamon Press, New York, 1960.

10. R. E. Walkerband A. A. Westenberg, J. Chem. Phys. 29, 1147 (1958).

11. R. L. Nuttall and D. C. Ginnings, J. Res. Natl. Bur. Stds. 58, 271 (1957).

12. D. W. Stops, Nature 164, 966 (1949).

13. R. G. Vines, J. Heat Trans. 82, 48 (1960).

14. A. J. Rothman and L. A. Bromley, Ind. Eng. Chem. 47, 899 (1955).

15. N. B. Vargaftic and O. N. Oleschuk, Izvest. VTI 15, Nos. 6, 7 (1946).

II. ROCKET NOZZLE FLUID DYNAMICS

(F. K. Hill and H. J. Unger)

Objective

The dynamics of high-speed gas flows in rocket nozzles has become increasingly important to the efficient utilization of high-energy solid propellants. The flow characteristics of the gas mixture are dependent on the thermodynamic properties of the components and certain time-dependent phenomena such as chemical reaction rates, recombination and condensation. Acquisition of the experimental data required for an accurate description of the gas flow from a relatively simple propellant and rocket nozzle combination has been the first objective.

In order to provide realistic and representative testing conditions for the experiment, a double-base solid propellant (ARP)* has been chosen which provides the basic constituents common to most high-impulse propellants. These are hydrogen, nitrogen, carbon monoxide, carbon dioxide and water vapor. Impurities of the order of 2 to 3% are present as is the case in all propellants and it is possible to add in well-controlled amounts and sizes solid particles for future extensions of the experimental studies. To begin with, it is believed advisable to keep the problems as uncomplicated as possible while still retaining the fundamental aspects of the phenomena under investigation. Combustion pressure and temperature of the grain are 1100 psi, nominal, and 2500°K, respectively, end burning is employed for either 10-second or 30-second operation. These conditions are sufficient to introduce measurable effects due to the variable gas properties as the gas expands through the nozzle, gas non-equilibrium conditions in the expanded flow

* The propellant is manufactured and proof-tested at Allegany Ballistics Laboratory.

and heat transfer and nozzle divergence angle effects. Associated phenomena, such as erosion and deposition of solid particles, are also present for observation providing additional data.

It is anticipated that as the work progresses higher specific impulse propellants will be utilized providing temperature in the 3000°K to 4000°K range, and that investigations will be undertaken of the effects of metal additives to the grain and some properties of materials as they are affected by the rocket gases.

Flow Separation Near the Nozzle Throat

In the previous progress report (Ref. 1) the results of two tests investigating separation in the nozzle throat region were described. The third test in this series was subsequently run to measure the pitot pressure distribution with the modified nozzle throat geometry. The pressures obtained indicated that a shock still existed near the axis at this station, but that the pressure rise in the shock-free region was smaller than occurred with the unmodified geometry. This substantiated the previous inference that the increased radius of the throat areas, providing a more gradual change in curvature to the conical surface, reduced or eliminated the separated region. The static wall and pitot pressures were constant throughout the run as compared to decreasing values in unmodified nozzle tests. It was concluded that the shock which remains in the modified nozzle was most likely due to a transition to turbulent flow which was further substantiated by the deposition of solid material on the wall surface downstream of the throat. These measurements thus clearly demonstrated that the arbitrary matching of a given conical expansion region to a throat contour generated by a circular arc may lead to appreciable deleterious effects in the usual nozzle configuration. For optimum performance and the minimizing of heat

transfer, this area should be contoured so as to provide a minimum discontinuity in the second derivative of the profile.

Auxiliary Settling Chamber

An auxiliary settling chamber with a molybdenum cup for obstructing particle movement was designed as described in the previous quarterly report (Ref. 1) and tested. The purpose of this chamber was to permit more quiescent gas conditions to obtain before entering the nozzle, to eliminate the radiant light from the propellant flame for optical studies, and to reduce the presence of solid particles which had led to erosion and roughening of test models and probes. Several tests were run with the above configuration and it was found that the system provided cleaner flow as evidenced by a much reduced erosion rate on probes and models and that there was a relatively small supply pressure drop. Some degradation in total temperature appeared, however, amounting to about 500°K.

Boundary Layer Measurements

In order to provide the fundamental data for heat transfer determination to the surface of rocket nozzles, it is necessary to know the detailed boundary layer characteristics under realistic flow conditions. Experimental measurements of the boundary layer were begun in the rocket tunnel with the probes and instrumentation developed earlier in the program. The measurements were made at a station where the Mach number was 4.5 and the Reynolds number, based on boundary layer thickness, was 5.2×10^4. The flow in the boundary layer was predominantly turbulent and of interest for direct comparison with turbulent boundary layer measurements made in hypersonic wind tunnels.

The data obtained come from three tests in which eight pitot probes were located peripherally around the section at varying distances

from the wall. For the probes close to the wall the tips were flattened by swaging and filing to provide an overall dimension of 0.024 in. with a minimum wall thickness of 0.003 in. The entire probe and shank assemblies were fabricated from molybdenum stock to eliminate any junctions or seals within the test section which would be exposed to the rocket gas. The results of the measurements are shown in Figures II-1 and II-2 which give typical pitot pressure data and the resulting Mach number distribution, respectively. These profiles, especially that shown in Figure II-2, indicate the predominantly turbulent characteristic of the flow from about 0.05 in. outward to the free stream and the laminar sub-layer at the wall. Experiments are now under way to survey the total temperature distribution in the boundary layer. With the total temperature data and the Mach number distribution, the static or stream temperature and the velocity profiles may be calculated. This will then provide all the needed information to compute both the heat transfer and skin friction coefficients at the wall. It is planned to make surveys at several axial locations in the nozzle and as far upstream as the environmental conditions will permit.

Spectroscopic Development

The development of an infrared spectrometer for the purpose of making quantitative determinations of the composition of the gas in the high-temperature rocket tunnel during operation has continued. In our previous report (Ref. 1) evidence was given of mechanical vibration troubles in the optical system of the spectrometer. The most likely offender appeared to be the Nernst glower support which consisted of sheet mica. The positioning of the image of the source on the entrance slit of the spectrometer was very critical due to the size of the image

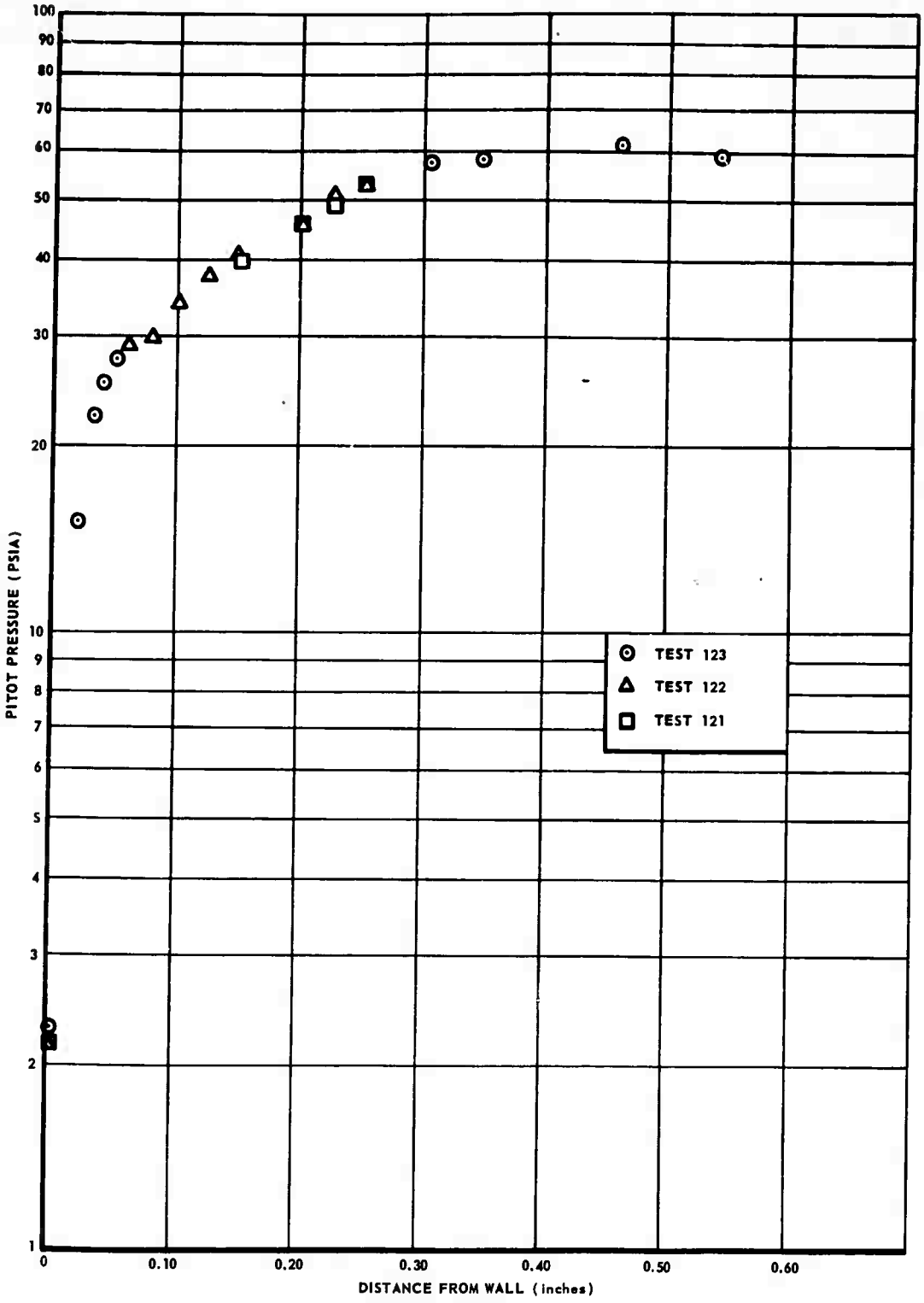

Fig. II-1 PITOT PRESSURE DISTRIBUTION IN THE BOUNDARY LAYER

Measurements were made on the inner nozzle surface at expansion ratio of 34, free-stream Mach number of 4.5. Data shown were obtained at 7 seconds in each test.

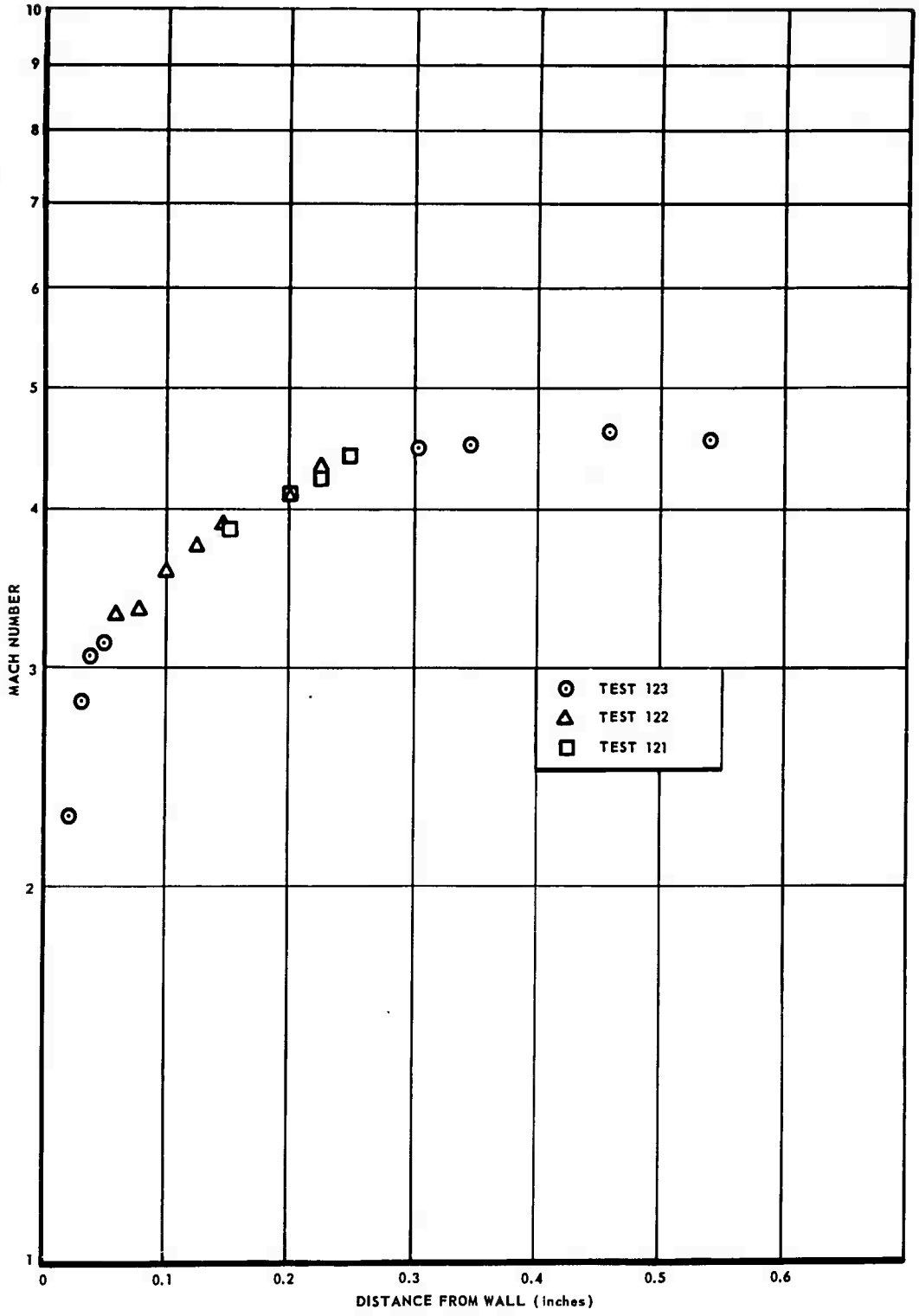

Fig. II-2 MACH NUMBER DISTRIBUTION OBTAINED FROM DATA GIVEN IN FIG. 1

Nozzle diameter at this station ~ 4 inches, total boundary layer thickness ~ 0.35 inches.

and the curvature of the slit. The small diameter (1/16") of the available Nernst glowers and the necessarily complicated collimating system made it impossible to avoid some amplitude modulation of the light source. The simplest solution to this difficulty was to increase the width of the source, and this has been done by incorporating a water-cooled globar which is ¼" x 5". The inconvenience of having to water cool the source mountings is offset by the mechanical stability of the light output.

It has been noticed that during tests with the rocket tunnel, when the spectrometer was in operation but not in the test cell, the airborne noise produced electrical noise in the recording system. By using a tape recording of the rocket noise, it was possible to subject the electronic system to a sound field up to 128 db with a 60 watt amplifier. This was sufficient to simulate the noise observed during test runs and the offending parts were found to be the first two stages in the tuned video amplifier. By shock mounting the tube sockets, weighting the tube shields with sheet lead, and selecting tubes, it was possible to eliminate all of the airborne noise effect at this sound level which was much higher than that encountered during test runs.

Another improvement that has been incorporated in the spectrometer is the replacement of the Au-Ge detector with a liquid nitrogen-cooled PbSe cell built to our specifications by Santa Barbara Research Center. This detector is about 10 times more sensitive at 4.2 μ and 5 times at 6.0μ than the Au-Ge cell previously used. However, if one wanted to extend the wavelength range beyond 6 μ , the Au-Ge cell is superior to the PbSe cell out to 9 μ.

In order to make absorption measurements at different wavelengths with equal accuracy, it is necessary to have the product of the

transmission factor of the spectrometer, the spectral sensitivity of the detector, and the spectral energy distribution times the effective slit width at the detector constant. This condition does not give any of the conventional conditions such as constant energy at the detector, but does allow one to make quantitative comparisons at the same wavelength. Our intention is to compare the absorption maximum of a band observed across the tunnel with that of a collected sample of the same gases at the same density at room temperature, as well as with a synthetic mixture.

An attempt was made to program the slits by cutting a cam that would give constant amplitude over the entire wavelength range. Figures II-3 and II-4 show the results of this programming and consist of the absorption spectrograms of the flushed and unflushed spectrometer path, respectively. The cam was designed experimentally by using a circular disc graduated in 10° steps with the radius of the disc chosen to give the desired slit width at 4 μ. The motor drive of the cam system was disconnected so that the cam could be set by hand at any desired wavelength. The slits were then opened by slipping a feeler gauge between the disc and the push rod that opens the slits simultaneously. By plotting the feeler gauge readings against the angular position, a graph was obtained of the desired cam. The first attempt to make the cam failed because 10° steps were too large and 0.001" accuracy in setting the milling machine table was too rough. In the second attempt to cut the cam, the feeler gauge readings were taken every 5° to the nearest 0.001" as before, but the graph was smoothed to the nearest 0.0001". The milling machine table motion was checked with a dial gauge independently of the drive screw. The resulting rough cam was then smoothed on a filing machine and finished with 10μ diamond dust on a

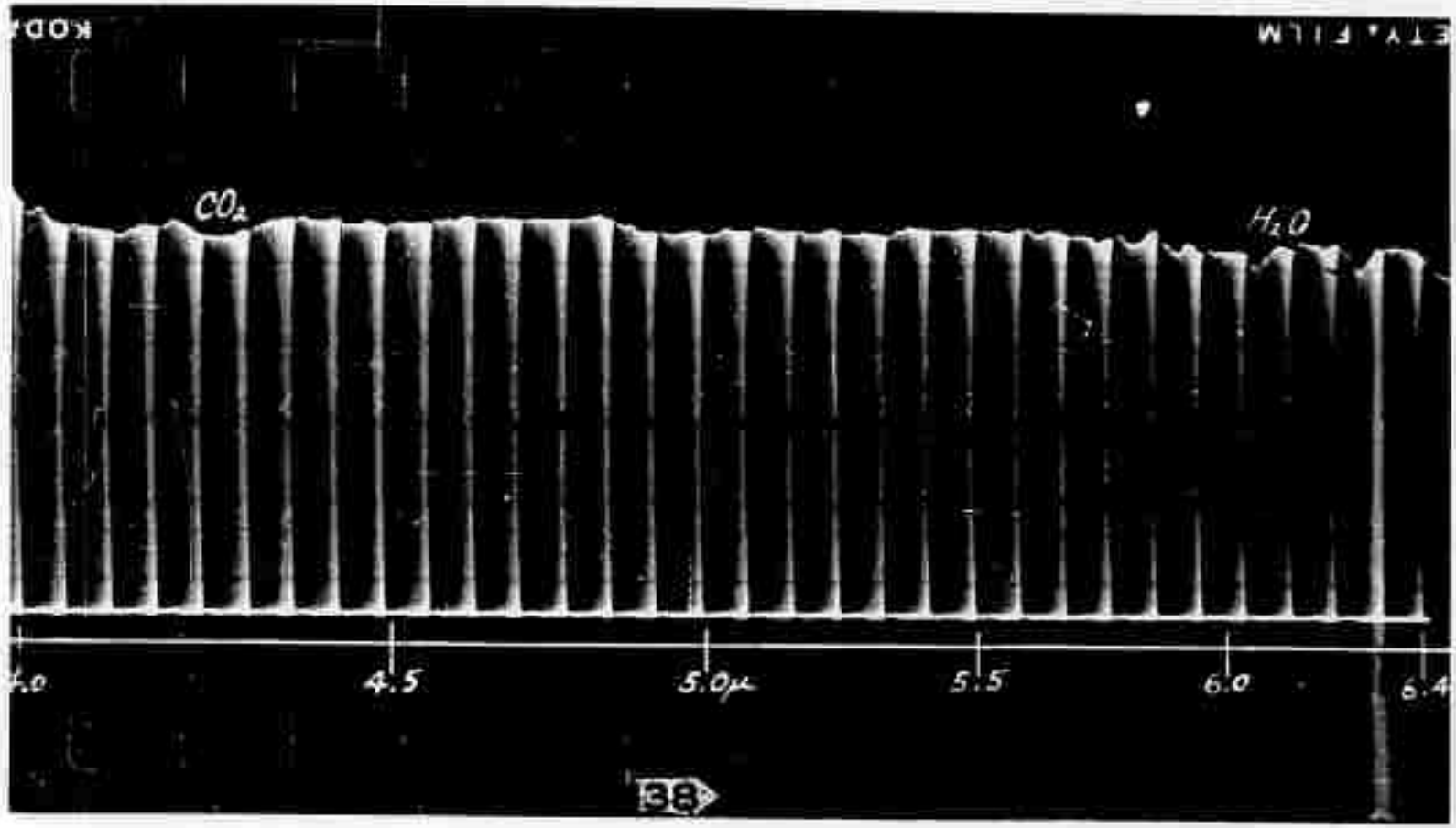

Fig. II-3 C.R.O. RECORD OF THE RESIDUAL ABSORPTION IN THE SPECTROMETER AND THE ABSORPTION CELL JUST BEFORE FIRING IN TEST NO. 125

Programmed slits for constant transmission with globar source at 3.80 amperes. The dark vertical lines are 10° markers on the cam axis and correspond to 0.0231 sec. on a time scale.

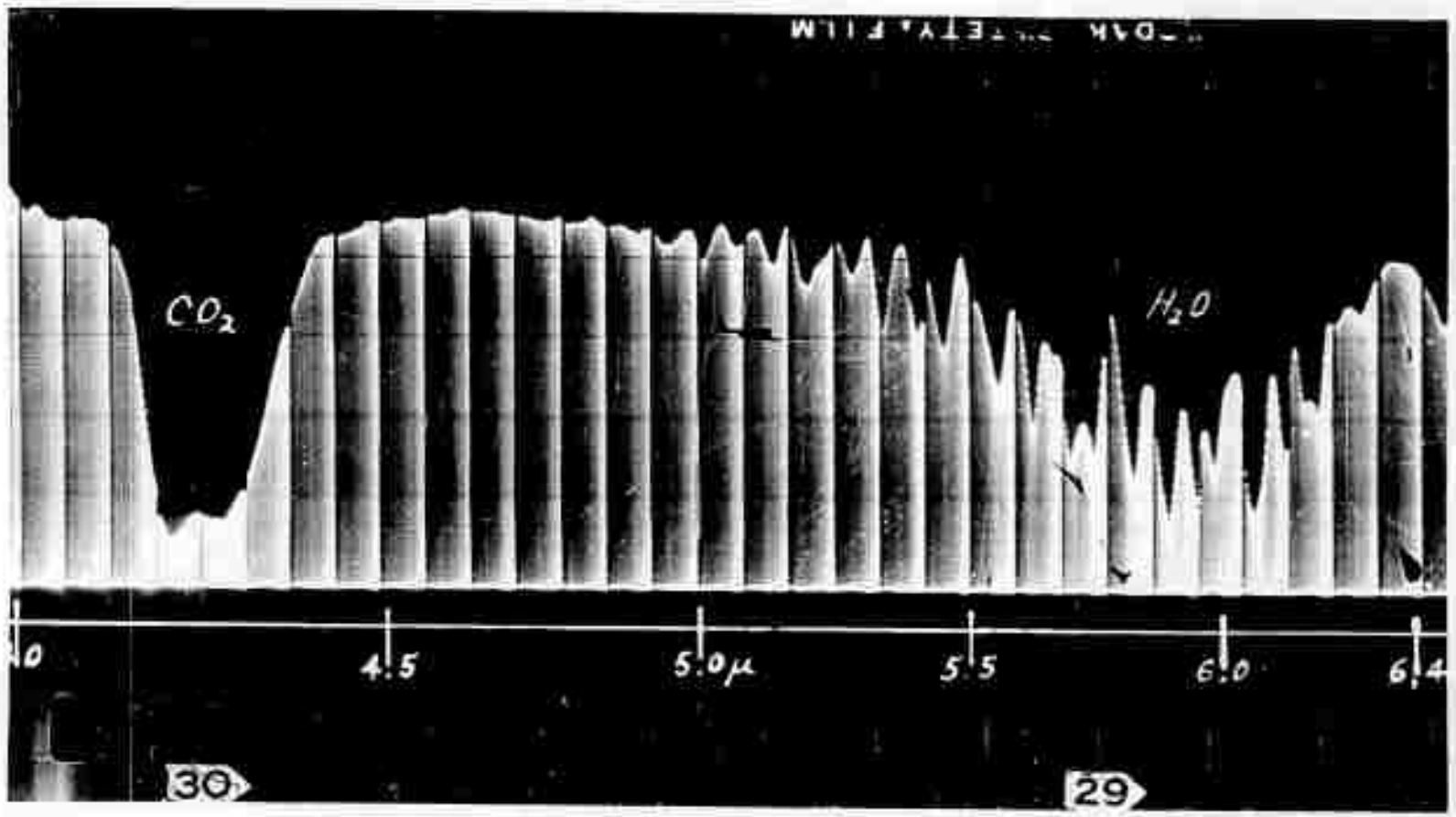

Fig. II-4 AMBIENT ATMOSPHERIC ABSORPTION
PbSe detector with programmed slits.

brass lapping tool. The final polishing was done by hand with the cam in operating position. The high spots were rubbed down with a fine oil stone until Fig. II-3 was obtained and, although there remain a few undulations of the order of 0.0001" on the cam, it was felt that the curve was sufficiently flat for the present requirements. The venetian blind effect on the spectrograms is due to the wavelength blanking signal applied to the C.R.O. beam every 10° of rotation of the wavelength cam.

Figure II-5 is a picture of the rapid scanning infrared spectrometer set in test position with rocket test section, "D", partially assembled to show details of the absorption cell. "A" and "B" are the massive optical benches which support the infrared source with its collimating unit, "C", and the spectrometer components, respectively. "E" is the combustion chamber with its loading breech, "F", removed. "G" is the housing for half of the collimating system which focuses an image of the light source on the entrance slit of the Perkin-Elmer monochromator, "H". "I" is the housing for the chopper disc which cuts the light beam just in front of the entrance slit at 1980 cps. "J" is a shield over the gear and cam assembly that oscillates the Littrow mirror and programs the slits. "K" is the detector assembly which houses the elliptical mirror that focuses the image of the exit slit on the detector. "L" is the sliding brass tube for focusing the light on the detector housed within. On the top of this tube is a plastic funnel for filling the Dewar with liquid nitrogen. "M" is the transistorized preamplifier for the video signal. All other amplifiers and recording equipment are located in another building. The "lectrodrier", "N", is used to dry the air that flushes the entire system. This removes the atmospheric CO_2 and H_2O from the light path except in the absorption cell. In actual operation the

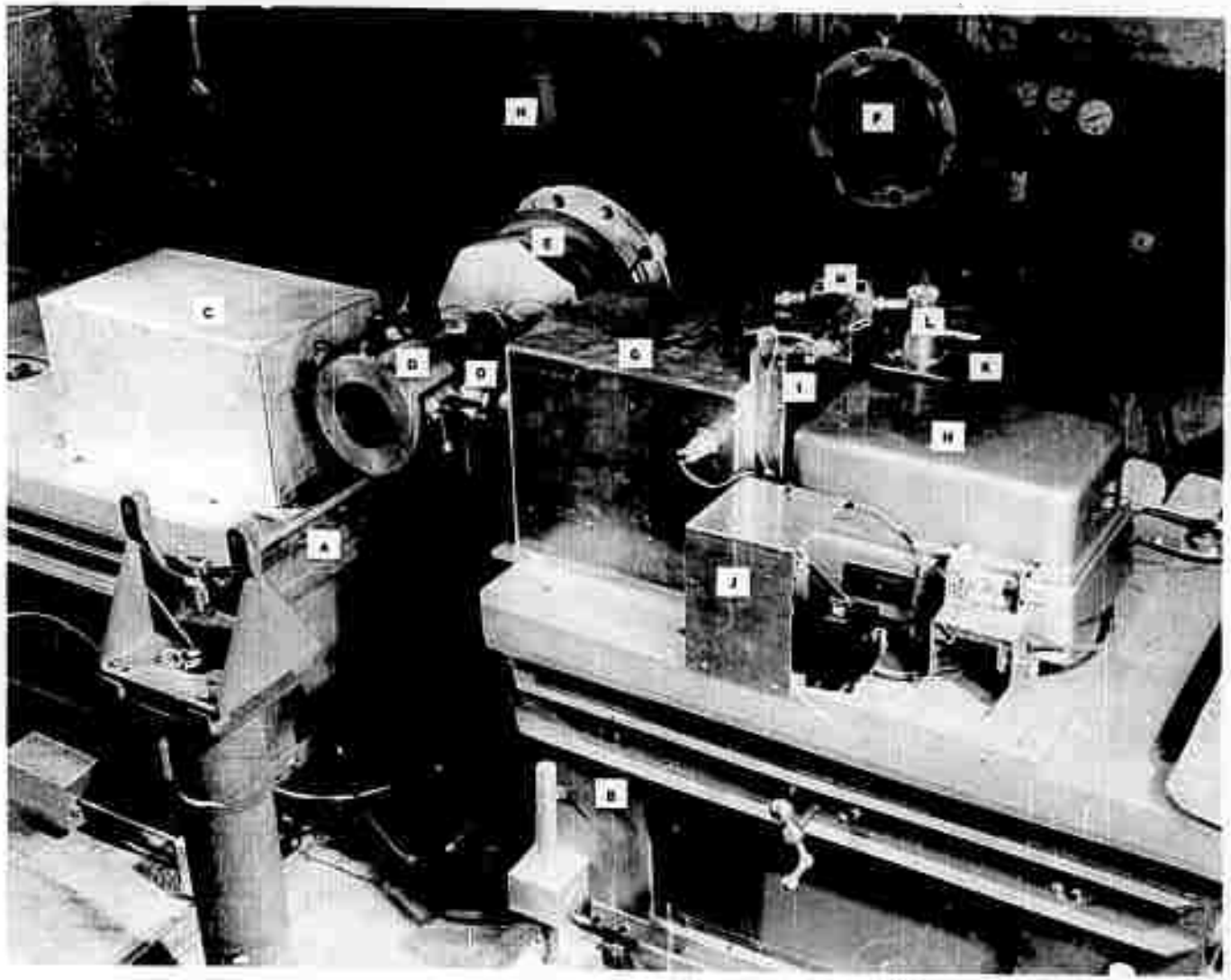

Fig. II-5 THE RAPID-SCANNING INFRARED SPECTROMETER IN TEST POSITION ON THE OPTICAL BENCHES

the CaF_2 crystal window housings, "O", are connected to the collimating boxes with flexible rubber tubes.

After all these improvements Test No. 125 was run with the axis of the absorption cell at station 3.5" from the nozzle exit. All previous tests had been made at station 5.0" with 0.8" circular holes through the cylindrical wall. At this station, fogging of the windows reduced the light transmission as much as 50% during a run and the side tubes were always coated with soot. In the new test section the openings in the conical wall at station 3.5" were made 5/16" wide and 1/2" high. This was done to reduce the possibility of having strong shockwaves across the absorption cell and to allow for better flushing of the CaF_2 windows.

Figure II-6 is a spectrogram taken during this test and, although the noise persists, it has changed in character. During the run there was no window fogging and inspection after the run showed no soot in the tubes.

The window fogging problem was solved but the noise problem lingers on. Before considering the noise problem, let us look at the absorption spectrum and compare it with previous tests.

In Figure II-6 the absorption of the 4.2 μCO_2 band is essentially the same as Figure III-10 of Ref. 1, but the 4.6μ CO band is extremely weak. No explanation of this discrepancy is offered at this time.

Figure II-7 shows an absorption spectrogram immediately after burn-out while still flushing the CaF_2 windows with dry nitrogen. The various oxides of nitrogen are observed due to the decomposition of the cellulose acetate inhibitor casing of the propellant. It was noted after the run that a part of this case had melted away after burn-out and that copious fumes of NO_2 (a red-brown gas) were issuing from the

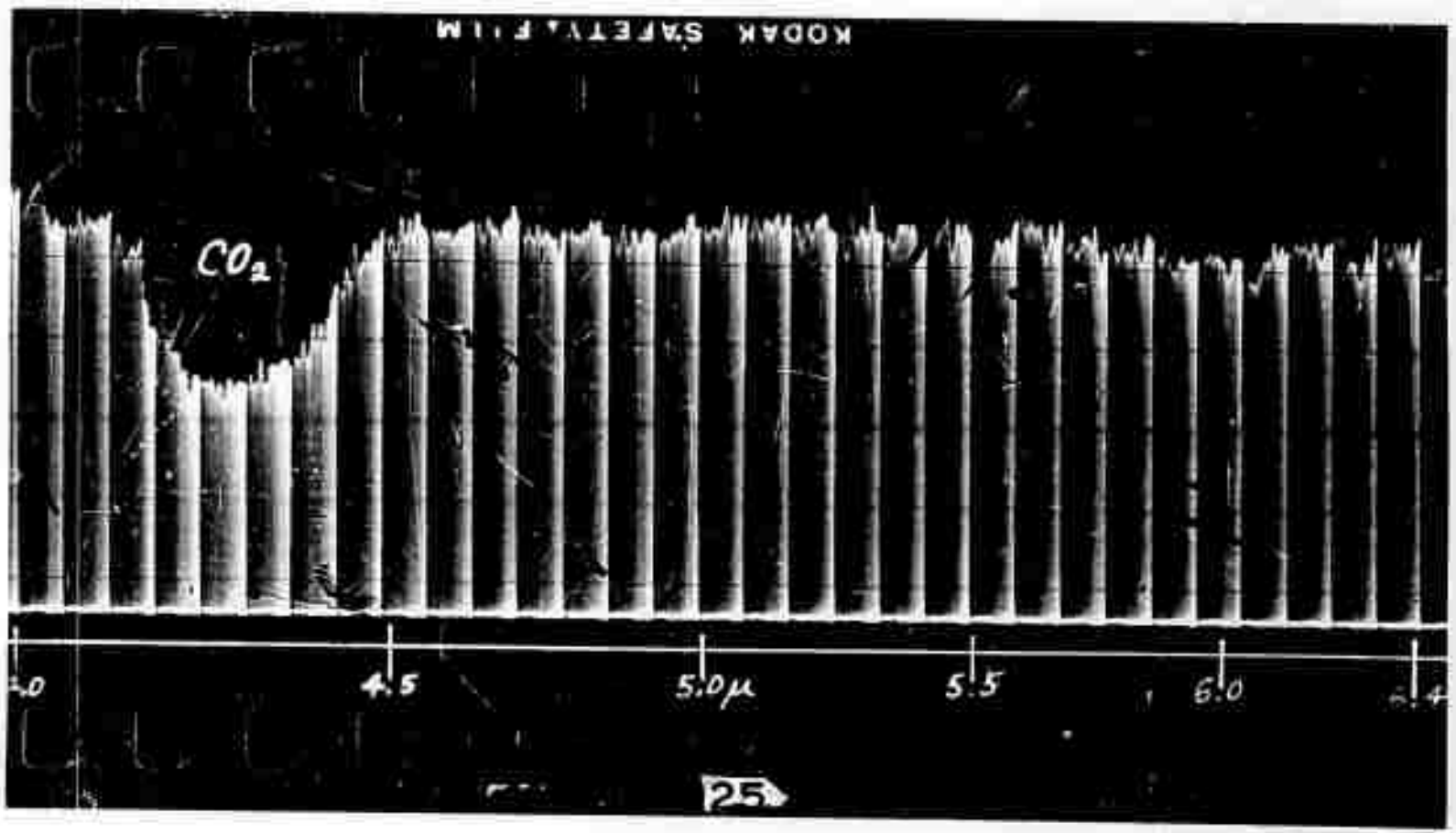

Fig. II-6 THE ABSORPTION SPECTRUM OF EXHAUST GAS IN THE WIND TUNNEL DURING TEST NO. 125

Absorption cell at station 3.5" on the 25° conical nozzle.

$T = 690\ °K$; $\rho = 4.6 \times 10^{-3}$ lbs/ft^3;

$P_s = 2.5$ lbs/in^2; $M = 4.42$.

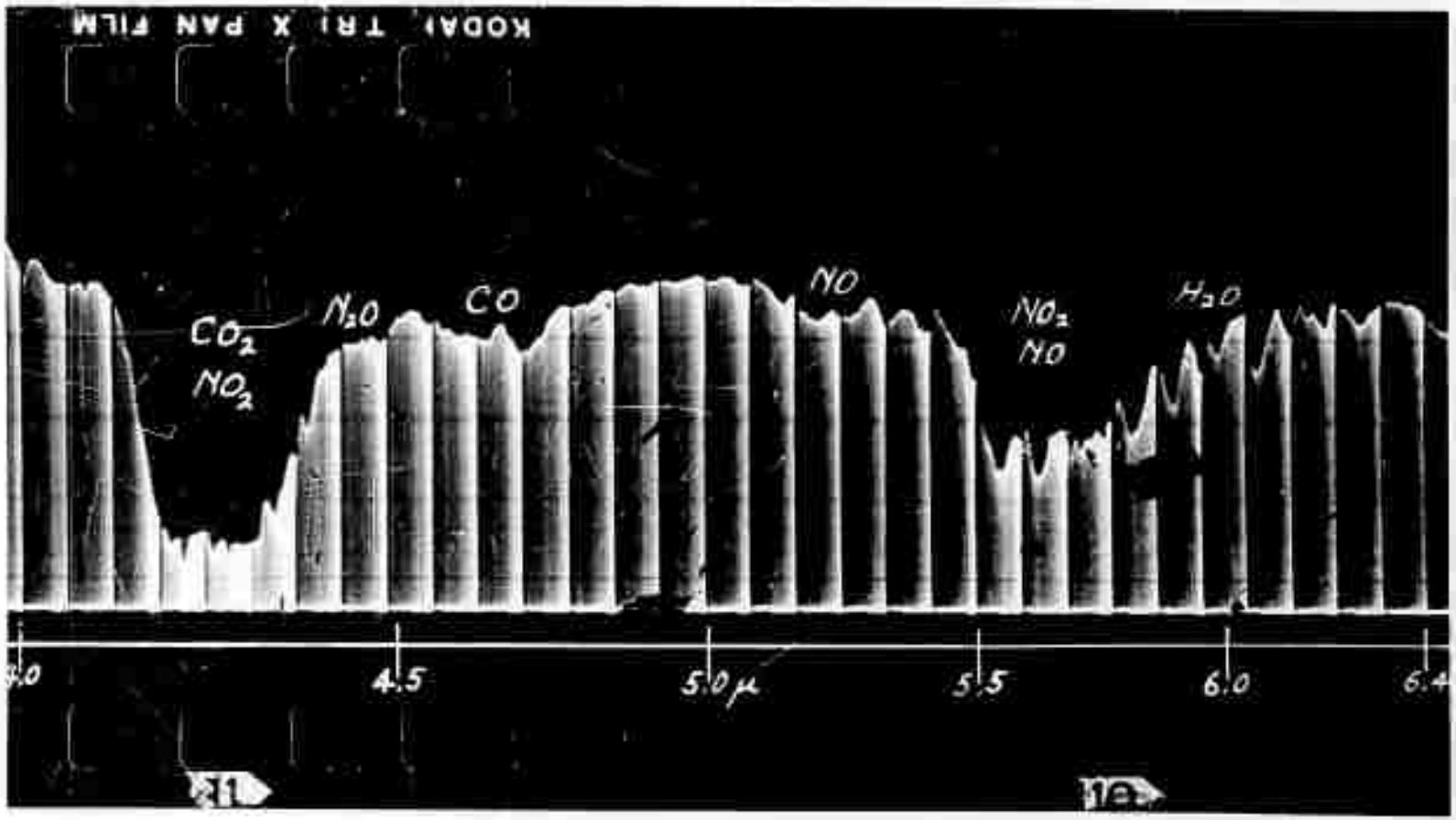

Fig. II-7 ABSORPTION SPECTRUM IMMEDIATELY AFTER BURN-OUT AT ATMOSPHERIC PRESSURE IN THE TUNNEL

The nitrogen oxides are from the disintegration of the cellulose acetate inhibitor case.

combustion chamber.

In Figure II-6 the two branches of the CO_2 band at 4.2μ overlap due to temperature broadening toward the long wavelength side so that they appear as one band. The broadening of the band is obvious when comparing it with the one in Figure II-4 taken at ambient temperature. In an article by C. Tingwaldt (Ref. 2) the absorption of this band was investigated at temperatures 300° - 1000°K and the broadening of the band was plotted. Measurements taken from Figures II-4 and II-6 show that the band broadens from 4.40μ at 300°K to 4.52μ which corresponds to 700°K according to Tingwaldt. The theoretical free-stream temperature at the observation station is 690°K.

The noise problem has been pursued and has been further isolated to the slit mechanism. Hammering the optical bench produces highly damped oscillations characteristic of opening the slits. Tapping the base of the spectrometer casting near the slit assembly produces the same effect, so it appears that the vibration problem is one or two steps nearer to solution.

No noise has been attributed to the detector and its mirror system. There was some apprehension as to how stable this detector would be in this severe environment since it has an F/3 radiation shield. The manufacturer did not guarantee the stability of the shield, but the latest version (#3) has the inner thimble of the Dewar, on which the detector and shield are mounted, supported by a plug of fibre glass between it and the outer glass wall. The Dewar is held in a fibre bakelite tube by two thin rubber washers. This makes a remarkably stable unit. It is felt that the vibration problem will soon be solved so that quantitative measurements may be made.

References

1. Task R Quarterly Progress Report No. 8, for the Period 1 January 31 March 1961. The Johns Hopkins University, Applied Physics Laboratory TG 331-8.
2. C. Tingwaldt, Physik Zeit 1, 1 (1939).

III. ROCKET NOZZLE CHEMICAL KINETICS

(A. A. Westenberg and S. Favin)

Objective

Aerodynamics and chemical kinetics are strongly coupled in the flow of most propellant gases through an exhaust nozzle. Understanding of this interaction and the ability to predict its effects must be founded solidly on the fundamental chemical processes involved. In all cases of practical importance, these basic processes are exceedingly complex. As a result, all of the theoretical work which has been done in this field has been confined to more-or-less idealized, simplified chemical systems - generally of the diatomic molecule dissociation-recombination variety. Even in these cases the analytical and computational problems are formidable, and various approximations have been proposed for dealing with the situation. The utility of these approximations in the more complex flows typical of real propellants remains to be established. The aim of this work is to apply the results of other phases of the Task R program, as well as work done elsewhere, and examine the complex chemical kinetics occurring in the flow of real propellant gases through nozzles with a view to determining if and when various simplifying procedures are valid.

Basic Equations for Numerical Calculations

In a previous quarterly report (Ref. 1), the equations governing the flow in a rocket nozzle with chemical reaction were presented in their most fundamental form. The discussion was appropriate to the particular nozzle and propellant being used in the experimental phase of this program (see Section II of the present report). It was shown that under the conditions

assumed for the nozzle inlet (T = 2500°K, P = 1150 psia), the only chemical species likely to be important were CO, CO_2, H_2, H_2O, H, OH, and N_2, and that these would participate in the reactions

$$\text{I.} \quad CO + OH \underset{k_{-1}}{\overset{k_1}{\rightleftharpoons}} CO_2 + H$$

$$\text{II.} \quad H + H_2O \underset{k_{-2}}{\overset{k_2}{\rightleftharpoons}} H_2 + OH$$

$$\text{III.} \quad H + H + M \underset{k_{-3}}{\overset{k_3}{\rightleftharpoons}} H_2 + M$$

$$\text{IV.} \quad H + OH + M \underset{k_{-4}}{\overset{k_4}{\rightleftharpoons}} H_2O + M$$

The rate constants for forward and reverse reactions are related to the equilibrium constant by (for example)

$$k_1 / k_{-1} = K_1; \quad k_3 / k_{-3} = K_3 RT$$

where k_1 and k_{-1} are in units of cm^3 $mole^{-1}$ $sec.^{-1}$, k_3 and k_{-3} in cm^6 $mole^{-2}$ sec^{-1}, and the equilibrium constants are defined in terms of partial pressures (atm.) by

$$K_1 = P_{CO_2} P_H / P_{CO} P_{OH}; \quad K_3 = P_{H_2} / P_H^2$$

The other constants are similarly defined.

The basic equations appropriate to the problem are as follows (the composition variable F_i is mole fraction divided by mean molecular weight of the mixture $\bar{M}$):

$$\frac{dF_{CO}}{dz} = \left(\frac{A}{A_t}\right)\left(\frac{A_t}{m}\right) \rho^2 k_1 \left[- F_{CO} F_{OH} + \frac{F_{CO_2} F_H}{K_1} \right] \tag{1}$$

$$\frac{dF_{H_2}}{dz} = \left(\frac{A}{A_t}\right) \left(\frac{A_t}{m}\right) \rho^2 \left[k_2 \left(F_{H_2O} F_H - \frac{F_{H_2} F_{OH}}{K_2} \right) + k_3 \sum F_i \left(\rho F_H^2 - \frac{F_{H_2}}{K_3 RT} \right) \right] \tag{2}$$

$$\frac{dF_{H_2O}}{dz} = \left(\frac{A}{A_t}\right)\left(\frac{A_t}{m}\right) \rho^2 \left[-k_2 \left(F_{H_2O} F_H - \frac{F_{H_2} F_{OH}}{K_2} \right) + k_4 \sum F_i \left(F_H F_{OH} - \frac{F_{H_2O}}{K_4 RT} \right) \right] \tag{3}$$

$$F_{CO_2} = \left(F_{CO_2} + F_{CO} \right)_o - F_{CO} \tag{4}$$

$$F_{OH} = \left(2F_{CO_2} + F_{CO} + F_{H_2O} + F_{OH} \right)_o - (2F_{CO_2} + F_{CO} + F_{H_2O}) \tag{5}$$

$$F_H = (2F_{H_2O} + 2F_{H_2} + F_{OH} + F_H)_o - (2F_{H_2O} + 2F_{H_2} + F_{OH}) \tag{6}$$

$$F_{N_2} = \left(F_{N_2} \right)_o \tag{7}$$

$$\frac{dP}{dz} + \rho v \frac{dv}{dz} = 0 \tag{8}$$

$$\frac{d}{dz} \left[\sum F_i H_i + \frac{v^2}{2J} \right] = 0 \tag{9}$$

$$P = \rho RT \sum F_i \tag{10}$$

$$\frac{m}{A_t} = \rho v \frac{A}{A_t} \tag{11}$$

These eleven equations are to be solved for the eleven dependent variables (seven F_i, P, T, ρ and v) it being presumed that the area ratio A/A_t (t = throat) is a known function of the distance coordinate z. The mass flow per unit throat area m/A_t is in the nature of an eigenvalue of the problem as we shall see. Its value must be assumed for each trial solution. The F_i as well as T and P are assumed known at the inlet (subscript o).

For actual numerical solution, the equations may be simplified further. The pressure P may be eliminated from the problem first by differentiating Eq. (10) with respect to z and combining with Eq. (8). This gives

$$v \frac{dv}{dz} = - R \left[T \sum \frac{dF_i}{dz} + \frac{dT}{dz} \sum F_i + \frac{T}{\rho} \frac{d\rho}{dz} \sum F_i \right] \tag{12}$$

If the indicated differentiation in Eq. (9) is carried out making use of the fact that for ideal gases molar enthalpies H_i are functions of T only so that

$$\frac{dH_i}{dz} = \frac{dH_i}{dt} \frac{dT}{dz} = C_i \frac{dt}{dz}$$

where C_i is molar heat capacity at constant pressure, we get

$$v \frac{dv}{dz} = - J \left(\frac{dT}{dz} \sum F_i C_i + \sum H_i \frac{dF_i}{dz} \right) \tag{13}$$

Differentiating Eq. (11) gives

$$\frac{1}{A/A_t} \frac{d(A/A_t)}{dz} + \frac{1}{\rho} \frac{d\rho}{dz} + \frac{1}{v} \frac{dv}{dz} = 0 \tag{14}$$

The velocity term $v(dv/dz)$ may now be eliminated between Eqs. (13) and (12), using (14), with the result that

$$\frac{dT}{dz} = \frac{J\left[\frac{1}{R\sum F_i} - T\rho^2\left(\frac{A}{A_t}\right)^2\left(\frac{A_t}{m}\right)^2\right]\sum H_i \frac{dF_i}{dz} + \frac{T}{A/A_t}\frac{d(A/A_t)}{dz}}{1 - J\left[\frac{1}{R\sum F_i} - T\rho^2\left(\frac{A}{A_t}\right)^2\left(\frac{A_t}{m}\right)^2\right]\sum F_i C_i} \qquad (15)$$

Then, eliminating $v(dv/dz)$ between Eqs. (14) and (12), we get

$$\frac{d\rho}{dz} = \rho^3\left(\frac{A}{A_t}\right)^2\left(\frac{A_t}{m}\right)^2\left[\frac{\frac{dT}{dz} - \frac{T}{A/A_t}\frac{d(A/A_t)}{dz}}{\frac{1}{R\sum F_i} - T\rho^2\left(\frac{A}{A_t}\right)^2\left(\frac{A_t}{m}\right)^2}\right] - \frac{\rho}{A/A_t}\frac{d(A/A_t)}{dz} \qquad (16)$$

The working equations have thus been reduced to nine in number - (1) through (7), (15) and (16) and the variables P and v eliminated. The sequence of events in the numerical solution may be summarized as follows: (i) At any point z_n in the nozzle where all conditions are known, Eqs. (1), (2), and (3) are used to compute the derivatives of F_{CO}, F_{H_2}, and F_{H_2O}. The quantities appearing on the right-hand side of these equations are all known functions of T (rate constants and equilibrium constants), z (the area function A/A_t), or assumed (the trial value of A_t/m). (ii) From these derivatives, new values of F_{CO}, F_{H_2O} at the next point $z_n + 1$ are obtained by a suitable integration scheme, and then from Eqs. (4) - (7) the new values of the remaining F_i. (iii) The temperature derivative at z_n is obtained from Eq. (15) and thus the value of T at z_{n+1}. (iv) Similarly, the value of $d\rho/dz$ at z_n is obtained from Eq. (16) using the dT/dz from Eq. (15), and then ρ at z_{n+1}. All the dependent variables are now known at the next point and the procedure begins again.

Throat Criterion

As mentioned above, the quantity A_t/m is an eigenvalue of the nozzle problem, i.e. there is only one value of A_t/m which will allow a smooth supersonic solution for a given set of inlet conditions (F_i, T, and P), kinetics constants, and geometry. The problem then arises as to how to correct A_t/m. In the case of "frozen" flow (isentropic), the criterion would be that the Mach number at the throat be unity, i.e.

$$\text{Mach No.} = \frac{v}{\sqrt{\bar{\gamma} RT \sum F_i}} \quad ; \qquad \bar{\gamma} = \frac{\sum F_i C_i}{\sum F_i C_i - R}$$

Similarly, in the "equilibrium" flow extreme (also isentropic) a Mach number can also be defined which involves an effective γ. The latter includes the effect of the shifting composition and is much more complex- for a case where the mean molecular weight is not constant it is prohibitively complex for practical use. Therefore, it is clear that the concept of a Mach number defined in this usual way is not a natural or convenient one. Instead, if one returns to the fundamental equations from which the Mach number was derived, the desired criterion is easily found. Thus, for <u>any flow whether isentropic or not</u>, Eqs. (14) and (8) may be combined to give

$$\frac{d(A/A_t)}{A/A_t} = \frac{dP}{\rho v^2} \left(1 - v^2 \frac{d\rho}{dP} \right)$$

For any A_t/m above the critical value, $dP = 0$ at the throat where $d(A/A_t) = 0$. But for the critical A_t/m where the flow passes from subsonic to supersonic and $dP \neq 0$, the relation.

$$v = \sqrt{dP/d\rho} \qquad (17)$$

must hold. Thus the criterion for a correctly chosen A_t/m is one for which Eq. (17) holds at the throat (to the desired precision). It will be recognized, of course, that in either the frozen or equilibrium isentropic flow extremes the right side of Eq. (17) would be written $\sqrt{(\partial P/\partial \rho)_s}$ which is also

identified with the sound velocity under these conditions. Eq. (17) is more generally useful, however,

Numerical Solutions.

The actual example of a complex chemically reacting nozzle flow being studied is taken from the solid propellant work being carried out experimentally in another phase of the Task R program (see Section II of this report). The inlet conditions calculated for chemical equilibrium of the given propellant combustion products at a chamber pressure of 1150 psia are

P_o = 1150 psia

T_o = 2500°K

ρ_o = 0.0092947139 g cm^{-3}

$\bar{M}_o$ = 24.373784

$\left(F_{CO}\right)_o$ = 0.016712684

$\left(F_{H_2}\right)_o$ = 0.0050861457

$\left(F_{H_2O}\right)_o$ = 0.0094785010

$\left(F_{CO_2}\right)_o$ = 0.0049351280

$\left(F_{OH}\right)_o$ = 0.000014076600

$\left(F_{H}\right)_o$ = 0.000040940000

$\left(F_{N_2}\right)_o$ = 0.0047602110

The chemical kinetic rate constants used were (Ref. 1).

$k_1 = 10^3 \exp(-10000/RT)$ cm^3 $mole^{-1}$ sec^{-1}

$k_2 = 10^{15} \exp(-25000/RT)$ cm^3 $mole^{-1}$ sec^{-1}

$k_3 = 5 \times 10^{21}/T^2$ cm^6 $mole^{-2}$ sec^{-1}

$$k_4 = 10^{23}/T^2 \qquad \text{cm}^6\ \text{mole}^{-2}\ \text{sec}^{-1}$$

The corresponding equilibrium constants were computed at 100° intervals from the basic thermodynamic data (Ref. 2).

The nozzle geometry was somewhat simplified mathematically from that reported previously (Ref. 1) but remained essentially the same for all practical purposes. The contraction section was taken to have a radius governed by an equation of parabolic form

$$r = 0.2591090\ (z - 2.702431)^2 + 0.8001031$$

$$(0 \leqslant z \leqslant 2.702431\ \text{cm})$$

For the expansion section, conical geometry was assumed of either 25° or 12.5° total angle

$$\left.\begin{aligned} r\ (25°) &= 0.2216900\ (z - 2.702431) + 0.8001031 \\ r\ (12.5°) &= 0.10952\ (z - 2.702431) + 0.8001031 \end{aligned}\right\} (z \geq 2.702431\ \text{cm})$$

The area ratio function A/A_t was then computed from these radius functions ($r_t = 0.8001031$ cm). The mathematical discontinuity at the throat caused by the two separate radius functions led to no difficulty.

The equations outlined in the preceding discussion were programmed for solution on an IBM-7090 computer. The simultaneous first order differential equations were integrated by an available routine employing a fourth order Adams-Moulton method (variable step-size) with Runge-Kutta starting procedure. Unfortunately, the complete non-equilibrium problem has so far resisted actual machine solution, the reason being not yet clear. The difficulty is in getting the solution started at the inlet, where, after one or two steps, the integration always "blows up". A great deal of effort has been spent in trying various cures for this malady without success so far. It seems likely that the trouble lies in the fact that one is looking

initially for very small changes in the variables - all of which are strongly coupled. It was thought at one time that, because the mixture was started from an equilibrium condition where all the bracketed quantities in Eqs. (1), (2), and (3) are zero, the difficulty was caused by extreme sensitivity near this singularity. However, attempted solutions where the initial conditions were arbitrarily selected gas mixtures not at equilibrium did not behave any better. Furthermore, simplified partial solutions such as will be described can be started from a state of chemical equilibrium with no problems at all, so that this does not appear to be the basic difficulty. Work on this is continuing.

The iteration procedure for finding the eigenvalue A_t/m may be illustrated by the results for the frozen flow case. Iteration is started at high values of the parameter A_t/m, which represent mass flow rates below critical and thus all give valid solutions (subsonic throughout, of course) with smooth approach to the throat. A series of such gradually decreasing values of A_t/m gives results for frozen flow as shown in the following table:

A_t/m (cm^2 sec g^{-1})	z (cm)	$v/\sqrt{dP/d\rho}$	
1.773100×10^{-3}	2.702431	0.98853627	
1.773000	2.702431	0.99169568	
1.772900	2.702431	0 99759115	
1.772894	2.702431	0.99857523	
1.772892	2.702431	0.99911441	Exact eigenvalue lies between these two
1.772890	2.7015790	0.99998782	

The throat lies at z= 2.702431. As A_t/m is decreased, the value of the critical quantity $v\sqrt{dP/d\rho}$ approaches closer to unity. The final line of the table shows how the solution starts to blow up when A_t/m is below the eigenvalue, since it is not possible to reach the throat at all before violent

oscillations begin. In this case the value $A_t/m = 1.772891 \times 10^{-3}$ would be accepted as the correct eigenvalue for our purposes.

Once the correct A_t/m is determined, there remains the question of getting the solution through the throat into the "supersonic" regime. The sensitivity of such calculations near the throat is well known, and sometimes presents a problem in numerical work of this general nature. The procedure we found most successful was to reduce the precision index of the integration routine (a parameter which represents essentially the extent to which extrapolated and corrected values of a variable are expected to agree) after the eigenvalue was found, until the solution would proceed smoothly through the throat with steadily decreasing T and ρ as desired. In this way the throat region was "skipped over", so to speak. If desired, a more precise solution in the expanding section of the nozzle could then be obtained by starting another calculation at a point slightly downstream of the throat with higher precision index.

In addition to the complete solution to this nozzle problem, i.e. including all four of the reactions I - IV as non-equilibrium processes, it is of interest to examine the behavior of various partial solutions. The main effect on the nozzle flow is determined by the degree to which reactions I and II take place during passage through the nozzle. The net effect of these two may be written as the water gas reaction.

$$CO + H_2O \longrightarrow CO_2 + H_2$$

which is exothermic by about 9.8 k cal/mole at 298°K. Since the above four species (plus the inert N_2) make up the overwhelming majority of the total gas, they largely determine the chemical energy effect even though the recombination reactions III and IV are much more energetic on a molar basis. The radicals H and OH are present in very small amounts, so that their effects

are only indirectly felt via their influence on reactions I and II.

One possible simplifying assumption is that the recombination reactions III and IV are always equilibrated. Under this condition, we have the relations

$$K_3 = P_{H_2} / P_H^2 \quad \text{or} \quad F_H = (F_{H_2} / K_3 \rho \ RT)^{\frac{1}{2}} \tag{18}$$

$$K_4 = P_{H_2O}/P_H P_{OH} \text{ or } F_{OH} = (F_{H_2O}/K_4) \ (K_3/\rho \ RTF_{H_2})^{\frac{1}{2}} \tag{19}$$

which must be satisfied throughout the expansion process. Equilibration of III and IV also implies equilibration of II, since

$$K_2 = P_{H_2} P_{OH}/P_H P_{H_2O} = K_3/K_4.$$

Thus the only rate equation remaining is that for reaction I, i.e. Eq. (1). Using Eqs. (18) and (19) in (1) gives

$$\frac{dF_{CO}}{dz} = \left(\frac{A}{A_t}\right)\left(\frac{A_t}{m}\right) \frac{\rho^{3/2} \ k_1}{(RT)^{\frac{1}{2}}} - \left[\frac{F_{CO} \ F_{H_2O}}{K_4} \left(\frac{K_3}{F_{H_2}}\right)^{\frac{1}{2}} + \frac{F_{CO_2}}{K_1} \left(\frac{F_{H_2}}{K_3}\right)^{\frac{1}{2}}\right] \tag{20}$$

This equation plus the element conservation equations (4) - (7) (F_H and F_{OH} can be set equal to zero in these equations for all practical purposes) and the usual Eqs. (15) and (16) are sufficient to solve the problem. This partial solution was numerically obtained with no trouble about starting whatsoever.

Another solution was obtained under the assumption of complete shifting equilibrium throughout the flow. This was done by means of a standard program available for computing equilibrium composition and temperature after isentropic expansion of a given mixture to any assigned pressure (Ref. 3). These equilibrium mixtures were then related to area ratios and nozzle axial positions z by appropriate use of Eqs. (9), (10), (11) and the geometry

functions. This was a complete equilibrium solution in that atoms and radicals (H and OH) were included, unlike the earlier equilibrium solution which considered only the water gas reaction (Ref. 4).

References

1. Task R Quarterly Progress Report No. 6 for the period 1 July - 30 September 1960. Applied Physics Laboratory, The Johns Hopkins University Report No. TG-331-6 (October 1960).

2. V. N. Huff, S. Gordon, and V. E. Morrell, NACA TR-1037 (1951).

3. H. N. Brown, M. M. Williams, and D. R. Cruise, NAVWEPS Report 7043 (June 1960).

4. Task R Quarterly Progress Report No. 5 for the period 1 April - 30 June 1960, Applied Physics Laboratory, The Johns Hopkins University Report No. TG-331-5 (July 1960).

The distribution of this document has been made in accordance with a list on file in the Technical Reports Group of the Applied Physics Laboratory, The Johns Hopkins University.

UNCLASSIFIED

UNCLASSIFIED